Detection of Carbon Nanotubes in Environmental Matrices Using Programmed Thermal Analysis

Kyle Doudrick[1*]; Pierre Herckes, Ph.D.[2]; Paul Westerhoff, Ph.D.[1]

[1]Arizona State University, School of Sustainable Engineering and The Built Environment, Tempe, AZ 85287-5306

[2]Arizona State University, Department of Chemistry and Biochemistry, Tempe, AZ 85287-1604

[*]**Corresponding Author:** Email: kdoudric@asu.edu

Total pages: 15

Tables: 2

Figures: 9

Supplemental Information

Carbon nanotube details. Carbon nanotubes (CNTs) are cylindrical and can be single-walled (SWCNT) or multi-walled (MWCNT). SWNTs are essentially a single sheet of graphite (called graphene) rolled up and connected end to end. MWCNTs are concentric SWCNTs of increasing diameter. Because of their unique properties, double-walled carbon nanotubes (DWCNTs) are considered a separate class of MWCNT. All CNTs have unique and excellent electrical, thermal, and physical properties with a high strength to weight ratio, which makes them ideal for a variety of applications [1]. The method of production affects the mechanical, electrical, and thermal properties of the CNTs [2]. Laser ablation is common for SWCNTs, and it produces CNTs similar to the Arc technique. Laser ablation is not currently used for large-scale production of MWCNTs.

The CVD process operates at low temperatures (<1000°C) to produce CNTs with a high defect density (i.e., disorder), and the arc process operates at much higher temperatures (>3000°C) to produce CNTs with a low defect density. Consequently, the CVD CNTs have a lower thermal stability and less desirable mechanical and electrical properties as compared with arc CNTs. For SWCNTs, a metal catalyst is necessary for synthesis, and the raw product can contain a high percentage of metal catalyst impurities, up to 50% of the total weight. When MWCNTs are synthesized using the arc process, no metal catalyst is required, and thus there is no metal contamination. Arc produces a low yield of CNTs, generally 20-60%; the remaining mass is fullerenes, multilayer polygonal carbon nanoparticles, graphitic nanoparticles, amorphous carbon nanoparticles, and, for SWCNTs, metal catalysts. Generally, before arc CNTs are used they are purified with a gas- or liquid-phase chemical treatment or through physical separation such as centrifugation or filtration [3]. Often CNTs are chemically treated to add

surface functional groups to make them hydrophilic or for particle supports. Unfortunately, chemical oxidation induces defects in the CNTs and decreases their thermal stability. Physical and chemical destruction of the bonds occurs when the sp^2 orbitals are transformed to sp^3 orbitals, which are represented by non-hexagonal polygons (e.g., a pentagon). Physical destruction includes folding, tearing, twisting, or stretching of the CNT structure, and chemical or thermal destruction includes oxidation of the CNT or breaking of the C-C bonds.

Three MWCNTs representing the CNT treatment process included a raw (MW-O), purified (MW-P), and functionalized (MW-F) MWCNT. The MW-Os were obtained from Cheaptubes, Inc., and were used as received. The MW-Ps are the MW-Os purified with dilute HNO_3 to remove metal and amorphous carbon impurities. The MW-Fs are the MW-Ps further treated using microwave-assisted acid treatment (HNO_3/H_2SO_4) to add functional groups to the surface to make them hydrophilic (5.27% –COOH, 0.03% $–SO_3$) [4]. FTIR analysis revealed that no oxygenated funcational groups were present for MW-O and MW-P. The zeta potential (pH 7) for MW-O, MW-P, and MW-F was -14.5, -8.73, and -50.30, respectively, which provides further evidence for the presence of oxygenated functional groups on MW-F. MWCNTs synthesized by the Arc method were obtained from Alfa Aesar in raw form and used as received (Cat. #42886). Two commercial functionalized MWCNTs were obtained from Cheaptubes, Inc. They contained –OH (MW-OH, 2.5%) and –COOH (MW-COOH, 3.7%) functionalities on the surface as listed by the manufacturer. MWCNTs that had similar properties but with varying diameters were obtained from Sigma Aldrich (Cat. #636835, 636509, 636525, 694185) to examine the thermal stability as a function of diameter. One Sigma Aldrich MWCNT (MW-15) was annealed (graphitized) under inert conditions at 2000°C to represent graphitized CNTs (MW-15G). Mitsui MWCNTs (MW-Mitsui) are commonly used in toxicology studies and were obtained from the

University of Rochester. Low-purity (as received) SWCNTs were obtained from Sigma Aldrich (Cat. #636797) and contained mixed chirality. Purified SWCNTs (>90% carbon, >75% SWCNTs, <10% Mo/Co) of >50% semiconducting chirality (6,5) were obtained from SouthWest NanoTechnologies, Inc.

Analytical method details. Samples were analyzed using an thermal optical transmittance (TOT) OC/EC instrument show in detail in Figure SI-1. As the sample is analyzed, the volatilized and combusted carbon travels to an oxidizing oven (MnO_2 catalyst at 870°C), where it is transformed into carbon dioxide (CO_2). The CO_2 passes through a methanator (Ni firebrick–supported catalyst) and is reduced to methane (CH_4). The CH_4 signal is measured using a flame ionization detector (FID). At the end of the sample run, a known mass of CH_4 is injected into the sample oven to calibrate the FID; this known mass is used for quantification. An external standard of sucrose is used to validate the instrument calibration.

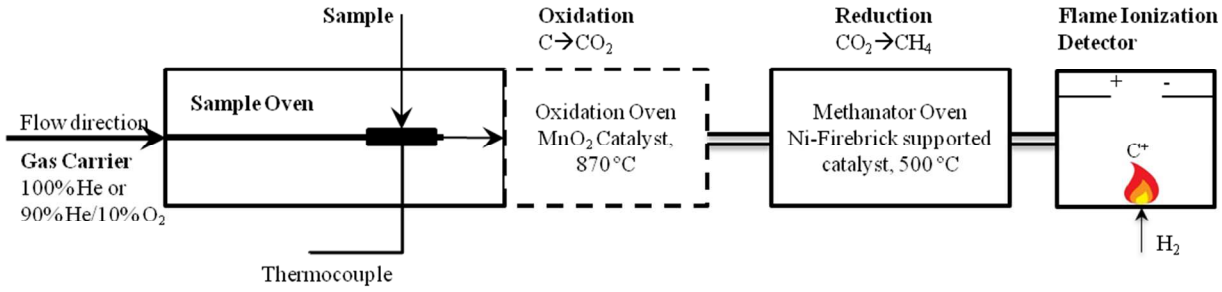

Figure SI-1. Instrument schematic

Samples are first heated under non-oxidizing conditions (100% He carrier gas) to remove volatile OC. The sample chamber is then cooled, switched to oxidizing conditions (90% He/10% O_2), and heated again. For this instrument, temperatures range from 0 to 920°C and are set by the user. OC that does not volatilize instead undergoes pyrolysis to become char or PEC, which has thermal properties similar to EC. Because the sample darkens as it chars and then lightens as the carbon evolves, optical correction is used to separate PEC (OC) from EC. A laser (632 nm) is

used to measure the transmittance or reflectance of the sample throughout analysis, and the split between OC and EC is automatically placed where the transmission returns to its original value after the char has been removed. Optical correction is only valid if the assumption that OC and PEC will evolve at lower temperatures than EC is true.

For this study, ultra-high purity gases were used, and an oxygen/moisture trap (Restek #20601) was put in line with the helium tank. QFFs are constructed of pure quartz and have a 99.9% aerosol retention efficiency for 0.3-μm particles according to the ASTM standard method, D2986-95a [5]. Because this study uses aqueous samples, the retention size cannot be used to estimate the nominal pore size, and thus the performance of these filters for aqueous samples is unknown. Upon use of QFFs to filter the aqueous CNT suspensions, which were well dispersed, a black filtrate was evident, and thus filtration through QFF was deemed a failure for this method.

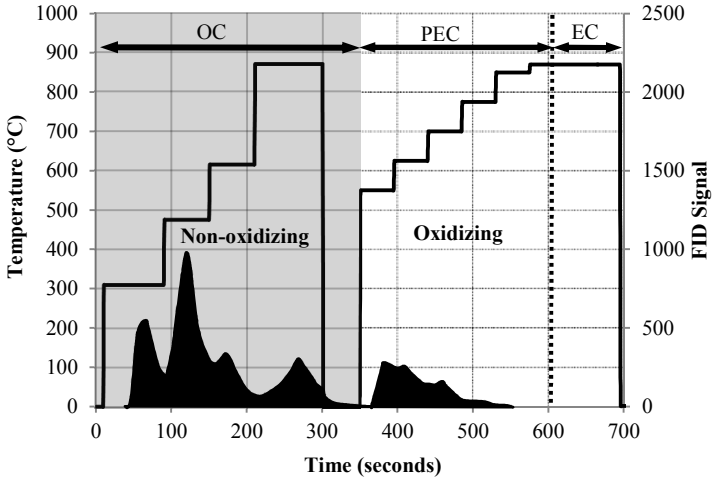

Figure SI-2. Thermogram example (sucrose) showing how OC, PEC, and EC are traditionally defined using the NIOSH temperature program. A 100% He carrier gas is used for non-oxidizing conditions, and a 90% He/10% O_2 carrier gas is used for oxidizing conditions.

Thermal optical analysis has been used frequently for analysis of black carbon in air and sediment samples, and because of the difficulty in analyzing black carbon against a carbon

matrix, there is no concurrence on analytical method that should be used [6, 7]. For high loadings of black carbon where the sample is too opaque to render a good optical reading, or non-homogenous filter loadings, such as with sediment samples, optical correction is not possible [6, 8]. We evaluated the validity of optical correction for MW-F CNTs using different split methods for OC/EC separation including two optical splits, transmittance and reflectance, and a manual split that was placed between the two carrier gas conditions. The manual split is considered valid on the basis of the assumption that when only CNTs are present, all carbon evolving under inert and oxidizing conditions is OC and EC, respectively. Maximum temperatures of 675°C and 910°C were used during inert and oxidizing conditions, respectively. The MW-F sample was used to evaluate the OC/EC split methods because it is relatively free of amorphous carbon (99.9% CNTs) and is assumed to be ~100% CNTs. A control filter (blank) showed that no OC/EC contamination was present owing to exposure of the filters to the air during drying. The manual gas split was placed between transitioning carrier gas conditions (i.e., 100% He to 90% He/10% O_2), and the automatic transmittance/reflectance splits were based on optical correction as determined by the laser reading and analytical software. The gas split provided the most reliable value; approximately 97% of the TC was defined as EC (i.e., CNTs). The mass lost during the non-oxidizing phase may be attributed to the oxygenated surface defects, as it is assumed there is no amorphous carbon remaining on the surface of the CNTs. If no loss had occurred during the non-oxidizing phase, 100% of the TC would be CNTs. The transmission and reflectance optical correction splits fared worse, retaining only 80% and 64% of the CNT mass, respectively. This was because the split was located where the CNTs evolved, due to a very low optical reading from the blackness of the CNTs. Therefore, this finding means that when

analyzing CNTs, a manual split, whether it is based on the carrier gases or a specified temperature, should be used.

Figure SI-3 shows a calibration curve for the MW-F stock solution for 2-100 μg, indicating a good analytical linear range. The method detection limit (MDL) for a weak CNT in a simple matrix was calculated using the EPA Method with nine replicates of MW-F CNTs in a tap water-X-114 mixture (~0.85%). Using a mean mass of approximately 3.70±0.25 μg, an MDL (99%) of approximately 0.72 μg was calculated. The lower critical limit (LCL) and the upper critical limit (UCL) for 95% confidence were calculated to be 0.30 μg and 1.02 μg, respectively. The limit of detection (LOD) and limit of quantitation (LOQ) were calculated to be approximately 1.8 μg and 2.5 μg, respectively.

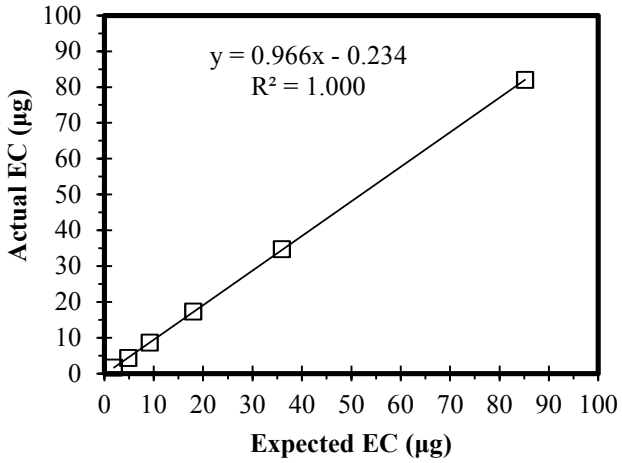

Figure SI-3. Calibration curve for MW-F CNT stock solution (0.85 g/L) using a manual gas split.

CNT Thermal Behavior

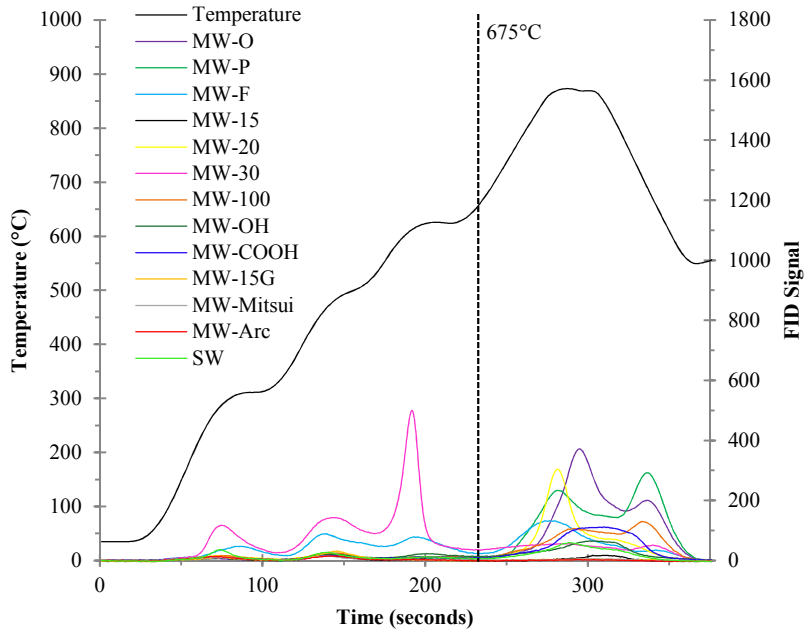

Figure SI-4. Thermograms of CNTs under non-oxidizing conditions using the NIOSH temperature program.

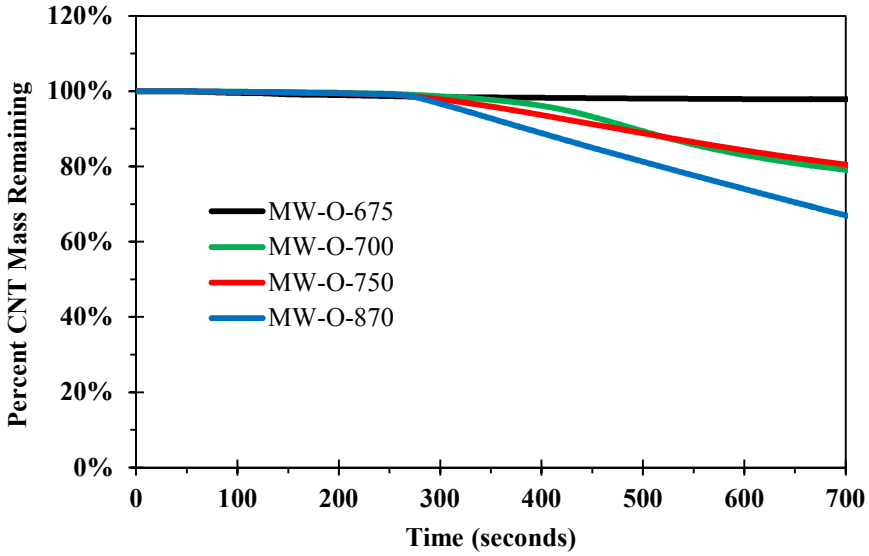

Figure SI-5. Percent MW-O mass remaining after analysis under non-oxidizing conditions at various maximum temperatures.

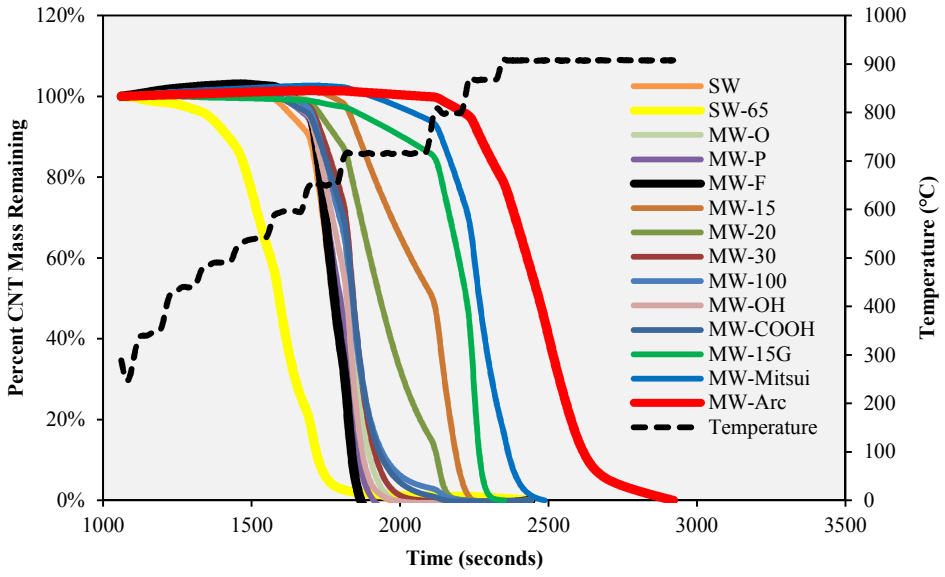

Figure SI-6. Mass loss curves of CNTs under oxidizing conditions.

Raman Spectroscopy. Figure SI-7a shows the Raman spectrograms of the D and G bands for a robust (MW-P) and a weak (MW-Arc) MWCNT. The robust MWCNT had a large D-band peak compared to the weak MWCNT, and its I_D/I_G ratio was much larger. SWCNTs (not shown) had similar ratios as the MW-Arc, but because SWCNTs are not as stable as the MW-Arc, the I_D/I_G ratio alone cannot be used to estimate the thermal stability of the CNTs in a sample. However, combined with the RBM (Figure SI-7b), Raman spectroscopy can be a powerful tool for characterization of the thermal stability of CNTs in an environmental or biological sample.

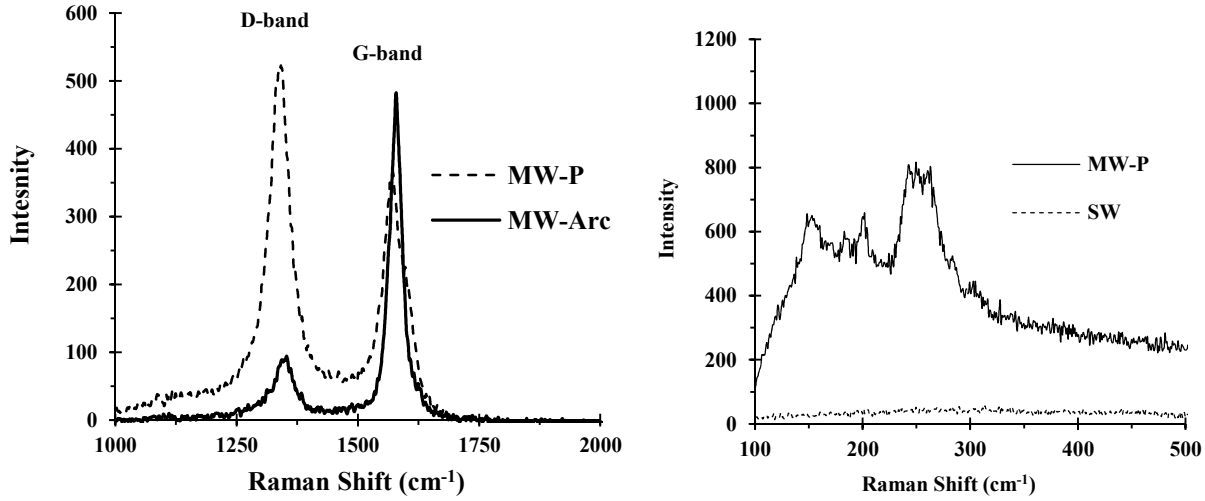

Figure SI-7. Raman spectroscopy of (a) MW-Arc and MW-P D-band and G-band peaks and (b) of the radial breathing mode for SWCNTs (SW) and MWCNTs (MW-P). SWCNTs (not shown) have a very similar D-band/G-band peak ratio as the MW-Arc.

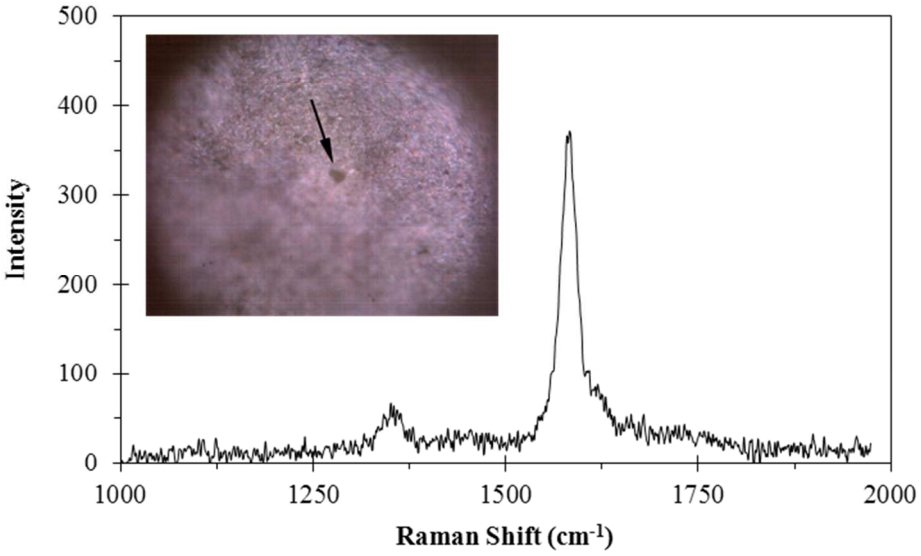

Figure SI-8. Raman spectroscopy of MW-Mitsui in a digest Cyanobacteria matrix loaded onto a quartz-fiber filter. Inset: Raman microscope image shows the CNT aggregate (indicated by arrow) used to gather the Raman spectrum.

(a)

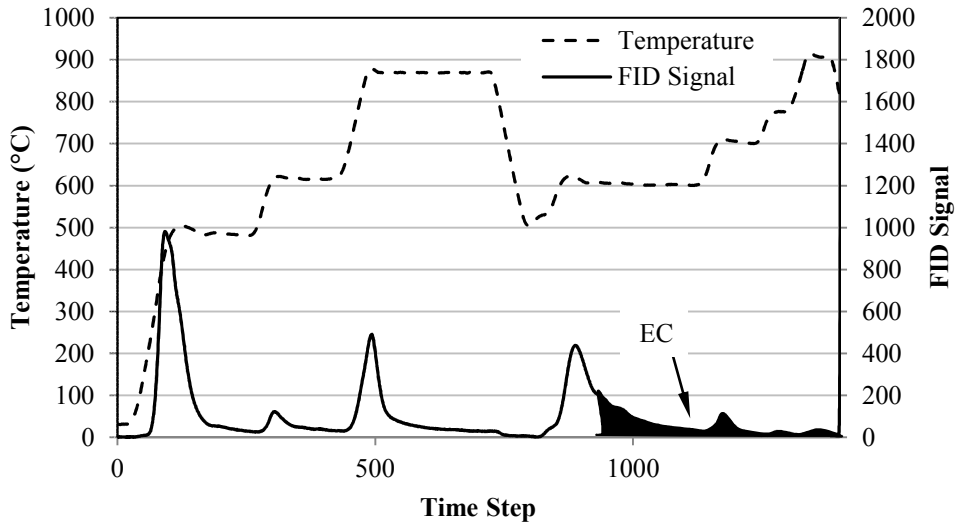

(b)

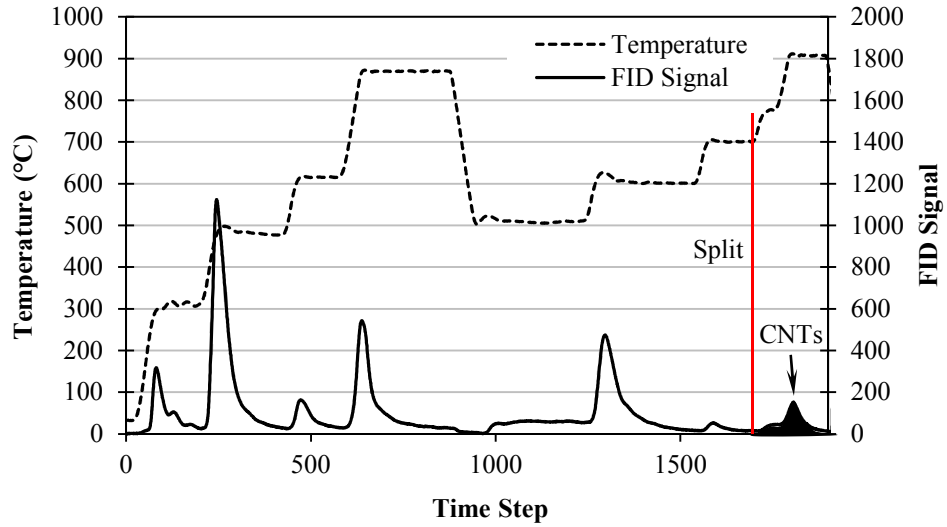

Figure SI-9. Thermograms of (a) urban air and (b) urban air spiked with 3 µg MW-Mitsui CNTs. The EC in (a) was determined by conventional air analysis using optical correction, and the CNTs in (b) by a manual split as discussed in this study.

Table SI-1. Quantification methods for carbon nanotubes

Method	Matrix	Application	Advantages	Disadvantages	Reference
Near-infrared fluorescence (NIRF)	Ultrapure water, D_20	Extracted SWCNT samples	Low detection limit ~1 µg	Only valid for semiconducting SWCNTs; CNTs must be fully dispersed; clean matrix only in D_2O	[9, 10]
Ultraviolet-visible light near infrared absorbance (UV-VIS NR)	Ultrapure water	Stock suspensions in water; extracted samples	Simple, economic, readily available	Clean matrix only with H_2O; good dispersion required	[11, 12]
Fluorescence probe labeling	Yeast cells	Toxicity studies; fate and transport	Excellent detection limit (2.5 fg); no background interferences; not biased to CNT type	Difficult; expensive; CNTs must be labeled first; may alter physicochemical surface properties	[13]
Isotopic labeling	Lumbriculus variegates Peat	Toxicity studies; fate and transport	Good for any type of matrix, no CNT bias	Difficult, expensive, isotope labeled CNTs must be used	[14, 15]
Gel electrophoresis	Tissue cells	Liquid samples	Very good detection limit (5 ng); no CNT bias	Low volume samples (60 uL max); internal calibration needed each time because of variation in gel, light intensity, and scan	[16, 17]
Thermogravimetric analysis (TGA)	CNT only	Characterization of dry CNTs	Simple, economic	Only valid for CNTs by themselves	[18]
Advanced[1] TGA coupled with MS (TGA-MS)	Marine sediments	Environmental matrices	Good separation of CNTs from organic and elemental carbon	Detection limit ~10 ug; complex instrument	[19]
Temperature programmed oxidation (TPO)	CNT only	Dry CNT samples	Simple, economic	CNT only matrix	[20, 21]
Chemothermal oxidation, 375 °C (CTO-375)	Marine sediments	CNTs in environmental matrices	Simple, economic, can separate CNTs from black carbon	Recovery is dependent on type of CNT (e.g., low for CNTs with high defect density	[22]

				and/or small diameter)	
Advanced[2] CTO	Rat lung tissue	Highly graphitic CNTs in complex matrices	Simple, economic, readily available	Can't distinguish between CNTs and carbon background unless a very stable CNT is used (i.e., low defect density)	[23]
Thermal optical transmittance (TOT)	CNT only, diesel particulate, NOM in water	Stock suspensions, CNTs in environmental matrices	Simple, economic, valid for all CNT types; good detection limit (1 µg); separation from black carbon	Optical separation only valid for homogeneously loaded samples	[24-26]

[1]Hydrogen assisted thermal degradation was used

[2]Pre-oxidative steps were employed to remove background organic/elemental carbon

Table SI-2. CNT ID/IG ratios and the temperature at 50% CNT mass loss under oxidizing conditions.

CNT ID	I_D/I_G	Oxidation Temperature (°C)[a]	CNT Thermal Classification
MW-O	1.3 ± 0.10	715	Thermally "Weak"
MW-P	1.4 ± 0.12	675	
MW-F	1.5 ± 0.12	650	
MW-15	0.78 ± 0.050	778	
MW-20	1.3 ± 0.10	716	
MW-30	1.2 ± 0.090	715	
MW-100	1.2 ± 0.16	715	
MW-OH	1.2 ± 0.18	717	
MW-COOH	1.2 ± 0.19	715	
SW	0.080 ± 0.060	651	
SG-65	0.13 ± 0.90	593	
MW-15G	0.52 ± 0.023	844	Thermally "Strong"
MW-Mitsui	0.10 ± 0.014	867	
MW-Arc	0.20 ± 0.060	907	

References

1. Aitken, R. J.; Chaudhry, M. Q.; Boxall, A. B. A.; Hull, M., Manufacture and use of nanomaterials: current status in the UK and global trends. *Occupational Medicine-Oxford* **2006,** *56*, (5), 300-306.
2. *Carbon Nanotubes: Science and Applications*. CRC Press LLC: Boca Raton, FL, 2005.
3. Hou, P. X.; Liu, C.; Cheng, H. M., Purification of carbon nanotubes. *Carbon* **2008,** *46*, (15), 2003-2025.
4. Wang, Y. B.; Iqbal, Z.; Mitra, S., Rapidly functionalized, water-dispersed carbon nanotubes at high concentration. *Journal of the American Chemical Society* **2006,** *128*, (1), 95-99.
5. ASTM Standard D2986-95a, 1999, "Standard practice for evaluation of air assaymedia by the monodisperse DOP (dioctyl phthalate) smoketest". In ASTM International: West Conshohocken, PA, 1999.
6. Hammes, K.; Schmidt, M. W. I.; Smernik, R. J.; Currie, L. A.; Ball, W. P.; Nguyen, T. H.; Louchouarn, P.; Houel, S.; Gustafsson, O.; Elmquist, M.; Cornelissen, G.; Skjemstad, J. O.; Masiello, C. A.; Song, J.; Peng, P.; Mitra, S.; Dunn, J. C.; Hatcher, P. G.; Hockaday, W. C.; Smith, D. M.; Hartkopf-Froeder, C.; Boehmer, A.; Luer, B.; Huebert, B. J.; Amelung, W.; Brodowski, S.; Huang, L.; Zhang, W.; Gschwend, P. M.; Flores-Cervantes, D. X.; Largeau, C.; Rouzaud, J. N.; Rumpel, C.; Guggenberger, G.; Kaiser, K.; Rodionov, A.; Gonzalez-Vila, F. J.; Gonzalez-Perez, J. A.; de la Rosa, J. M.; Manning, D. A. C.; Lopez-Capel, E.; Ding, L., Comparison of quantification methods to measure fire-derived (black/elemental) carbon in soils and sediments using reference materials from soil, water, sediment and the atmosphere. *Global Biogeochemical Cycles* **2007,** *21*, (3), 18.
7. Watson, J. G.; Chow, J. C.; Chen, L.-W. A., Summary of Organic and Elemental Carbon/Black Carbon Analysis Methods and Intercomparisons. *Aerosol and Air Quality Research* **2005,** *5*, (1), 65-102.
8. Schmid, H.; Laskus, L.; Abraham, H. J.; Baltensperger, U.; Lavanchy, V.; Bizjak, M.; Burba, P.; Cachier, H.; Crow, D.; Chow, J.; Gnauk, T.; Even, A.; ten Brink, H. M.; Giesen, K. P.; Hitzenberger, R.; Hueglin, C.; Maenhaut, W.; Pio, C.; Carvalho, A.; Putaud, J. P.; Toom-Sauntry, D.; Puxbaum, H., Results of the "carbon conference" international aerosol carbon round robin test stage I. *Atmospheric Environment* **2001,** *35*, (12), 2111-2121.
9. O'Connell, M. J.; Bachilo, S. M.; Huffman, C. B.; Moore, V. C.; Strano, M. S.; Haroz, E. H.; Rialon, K. L.; Boul, P. J.; Noon, W. H.; Kittrell, C.; Ma, J. P.; Hauge, R. H.; Weisman, R. B.; Smalley, R. E., Band gap fluorescence from individual single-walled carbon nanotubes. *Science* **2002,** *297*, (5581), 593-596.
10. Huang, H.; Zou, M.; Xu, X.; Liu, F.; Li, N.; Wang, X., Near-infrared fluorescence spectroscopy of single-walled carbon nanotubes and its applications. *TrAC Trends in Analytical Chemistry* **2011,** *30*, (7), 1109-1119.
11. Bahr, J. L.; Mickelson, E. T.; Bronikowski, M. J.; Smalley, R. E.; Tour, J. M., Dissolution of small diameter single-wall carbon nanotubes in organic solvents? *Chemical Communications* **2001**, (2), 193-194.
12. Li, Z. F.; Luo, G. H.; Zhou, W. P.; Wei, F.; Xiang, R.; Liu, Y. P., The quantitative characterization of the concentration and dispersion of multi-walled carbon nanotubes in suspension by spectrophotometry. *Nanotechnology* **2006,** *17*, (15), 3692-3698.
13. Xiao, H.; Zou, H. F.; Pan, C. S.; Jiang, X. G.; Le, X. C.; Yang, L., Quantitative determination of oxidized carbon nanotube probes in yeast by capillary electrophoresis with laser-induced fluorescence detection. *Analytica Chimica Acta* **2006,** *580*, (2), 194-199.
14. Petersen, E. J.; Huang, Q. G.; Weber, W. J., Bioaccumulation of radio-labeled carbon nanotubes by Eisenia foetida. *Environmental Science & Technology* **2008,** *42*, (8), 3090-3095.
15. Zhang, L. W.; Petersen, E. J.; Huang, Q. G., Phase Distribution of C-14-Labeled Multiwalled Carbon Nanotubes in Aqueous Systems Containing Model Solids: Peat. *Environmental Science & Technology* **2011,** *45*, (4), 1356-1362.

16. Wang, R. H.; Mikoryak, C.; Chen, E.; Li, S.; Pantano, P.; Draper, R. K., Gel Electrophoresis Method to Measure the Concentration of Single-Walled Carbon Nanotubes Extracted from Biological Tissue. *Analytical Chemistry* **2009,** *81*, (8), 2944-2952.
17. Wang, R. H.; Mikoryak, C.; Li, S. Y.; Bushdiecker, D.; Musselman, I. H.; Pantano, P.; Draper, R. K., Cytotoxicity Screening of Single-Walled Carbon Nanotubes: Detection and Removal of Cytotoxic Contaminants from Carboxylated Carbon Nanotubes. *Molecular Pharmaceutics* **2011,** *8*, (4), 1351-1361.
18. Pang, L. S. K.; Saxby, J. D.; Chatfield, S. P., Thermogravimetric analysis of carbon nanotube and nanoparticles. *Journal of Physical Chemistry* **1993,** *97*, (27), 6941-6942.
19. Plata, D. L.; Reddy, C. M.; Gschwend, P. M., Thermogravimetry-mass spectrometry for carbon nanotube detection in complex mixtures. *Enviornmental Science & Technology* **Submitted 2011**.
20. Alvarez, W. E.; Kitiyanan, B.; Borgna, A.; Resasco, D. E., Synergism of Co and Mo in the catalytic production of single-wall carbon nanotubes by decomposition of CO. *Carbon* **2001,** *39*, (4), 547-558.
21. Herrera, J. E.; Resasco, D. E., In situ TPO/Raman to characterize single-walled carbon nanotubes. *Chemical Physics Letters* **2003,** *376*, (3-4), 302-309.
22. Sobek, A.; Bucheli, T. D., Testing the resistance of single- and multi-walled carbon nanotubes to chemothermal oxidation used to isolate soots from environmental samples. *Environmental Pollution* **2009,** *157*, (4), 1065-1071.
23. Tamura, M.; Inada, M.; Nakazato, T.; Yamamoto, K.; Endo, S.; Uchida, K.; Horie, M.; Fukui, H.; Iwahashi, H.; Kobayashi, N.; Morimoto, Y.; Tao, H., A determination method of pristine multiwall carbon nanotubes in rat lungs after intratracheal instillation exposure by combustive oxidation-nondispersive infrared analysis. *Talanta* **2011,** *84*, (3), 802-808.
24. Myojo, T.; Oyabu, T.; Nishi, K.; Kadoya, C.; Tanaka, I.; Ono-Ogasawara, M.; Sakae, H.; Shirai, T., Aerosol generation and measurement of multi-wall carbon nanotubes. *Journal of Nanoparticle Research* **2009,** *11*, (1), 91-99.
25. Hyung, H.; Fortner, J. D.; Hughes, J. B.; Kim, J. H., Natural organic matter stabilizes carbon nanotubes in the aqueous phase. *Environmental Science & Technology* **2007,** *41*, (1), 179-184.
26. Ono-Ogasawara, M.; Serita, F.; Takaya, M., Distinguishing nanomaterial particles from background airborne particulate matter for quantitative exposure assessment. *Journal of Nanoparticle Research* **2009,** *11*, (7), 1651-1659.